DEPARTMENT OF THE NAVY
DAVID TAYLOR MODEL BASIN

HYDROMECHANICS

AERODYNAMICS

STRUCTURAL MECHANICS

APPLIED MATHEMATICS

TESTS OF MACHINED DEEP SPHERICAL SHELLS UNDER EXTERNAL HYDROSTATIC PRESSURE

by

Martin A. Krenzke

STRUCTURAL MECHANICS LABORATORY

RESEARCH AND DEVELOPMENT REPORT

May 1962

Report 1601

TESTS OF MACHINED DEEP SPHERICAL SHELLS UNDER EXTERNAL HYDROSTATIC PRESSURE

by

Martin A. Krenzke

May 1962

Report 1601
S-F013 03 02

TABLE OF CONTENTS

LIST OF FIGURES

LIST OF TABLES

ABSTRACT

Twenty-six structural models, consisting of hemispherical shells bound by ring-stiffened cylinders designed to provide ideal edge conditions, were machined from two aluminum alloys and collapsed under hydrostatic pressure. The models were designed to investigate both elastic and inelastic failures. The collapse pressure of those models which failed elastically could not be predicted by either the linear theory of Zoelly or any of the available large-deflection theories. When an empirical formula based on the observed elastic collapse pressures was used, the collapse pressure of those models which failed at stress levels above the proportional limit of the material could be predicted with reasonable accuracy. The agreement between the experimental values and those obtained from this empirical formula is within + 2 and - 12 percent.

INTRODUCTION

Underwater vehicles with positive buoyancy will be used at increasingly greater depths in the future. A strong possibility exists that these vehicles will utilize spherical shells either as the main pressure hull or, more likely, to close off the ends of basically cylindrical or spheroidal hulls.

Adequate design procedures do not exist for spherical shells.[1] Theoretical work carried out thus far has had little design value for underwater vehicles, since the majority of the efforts have been directed toward shallow spherical caps. In practice, the designer is likely to encounter deep or possibly complete spherical shells. The small amount of experimental data on the strength of deep or complete spherical shells found in the literature were obtained from shells much thinner than those of interest to the submarine designer. Since most materials considered promising for deep-depth application, such as high-strength steel and titanium and aluminum alloy, exhibit strain-hardening characteristics, knowledge of both the elastic and inelastic behavior of full or deep spherical shells made of such materials is required.

In an effort to shed light on the actual behavior of deep spherical shells, 26 small structural models were machined from two aluminum alloys and tested under external hydrostatic pressure. Because of the difficulty

---

[1] References are listed on page 25.

involved in constructing complete spherical shells with a high degree of accuracy, the models consisted of hemispheres bounded by stiffened cylinders designed to provide ideal membrane edge conditions. Models were designed to collapse in both the elastic and the inelastic ranges. This report describes the design, machining, test procedures, and results, and presents an empirical method for calculating the collapse pressures for machined spherical shells not affected by boundary conditions.

BACKGROUND

The small deflection theory for the elastic buckling of spherical shells was first developed by Zoelly in 1915 and summarized by Timoshenko.[2] If the average stress σ_1 of a spherical shell at the critical buckling pressure p_1 is defined by

$$\sigma_1 = \frac{p_1 R}{2h} \qquad [1]$$

(where R is the radius to the mean surface of the shell and h is the shell thickness), the classical linear theory for the buckling stress may be expressed by

$$\sigma_1 = \frac{E\, h/R}{\sqrt{3(1-\upsilon^2)}} \qquad [2]$$

where E is Young's modulus and υ is Poisson's ratio for the shell material. For Poisson's ratio of 0.3, the expression for the classical critical buckling pressure of a spherical shell becomes

$$p_1 = 1.21\, E\, (h/R)^2 \qquad [3]$$

Unfortunately, the very limited experimental data existing for deep spherical shells do not support the linear theory. Sechler and Bollay[1] immersed a brass hemispherical shell in a mercury bath and obtained an elastic-buckling load of about one fourth that predicted by the classical theory of Zoelly. Klöppel and Jungbluth[3] obtained similar results for deep spherical steel shells.

Various investigators have attempted to lower the theoretical elastic-buckling load of spherical shells to support experimental results. Von Kármán and Tsien[4] investigated the nonlinear buckling equations and the associated postbuckling equilibrium configurations. They determined the minimum load required to keep an elastic shell in the postbuckle position of finite deformations and offered this minimum value as the "lower" buckling load. Furthermore, they suggested that this lower buckling load would correspond more closely to the experimental values obtained from tests of spherical shells with imperfections and tolerances encountered in normal engineering practice, whereas the "upper" buckling load of Zoelly could be approached experimentally only by exercising extreme caution in the manufacturing and testing of the specimen. Their lower buckling pressure p_2 may be expressed as

$$p_2 = 0.366\ E\ (h/R)^2 \qquad [4]$$

This buckling pressure is in much better agreement with the existing experiments. Friedrichs[5] demonstrated, however, that relaxing several of the arbitrary assumptions made by Von Kármán and Tsien affects the results appreciably. In addition, Murray and Wright[6] have shown recently that a more exact mathematical solution to the equations of equilibrium of Von Kármán and Tsien[3] gives considerably higher collapse pressures. Tsien[7] later developed an "energy criterion of jump" which predicts elastic buckling pressures under dead-weight load conditions of about one fourth those obtained from the classical theory.

Bijlaard,[8] Gerard,[9] and Lunchick[10] have developed solutions for the inelastic buckling of spherical shells. Each followed the same basic approach of applying a plasticity reduction factor to the classical linear theory. Inadequate experimental data are available with which to check the validity of their work. It appears reasonable to assume, however, that an understanding of the elastic-buckling phenomenon would simplify the task of determining the inelastic strength of deep spherical shells.

Results of several simple tests on plastic spherical shells under uniform hydrostatic pressure are presented in the Appendix. These results indicate that the volume of the pressure vessel does not affect the experimental collapse strength, as implied by Tsien.[7] This leads to the speculation

that the observed difference between experiment and the classical theory must be the result of initial imperfections, residual stresses, and adverse boundary conditions. If this hypothesis is correct, the experimental collapse strength of near perfect, initially stress-free spherical shells should be higher than for imperfect shells.

It is evident that considerable experimentation is necessary in both the elastic and inelastic ranges before the collapse strength of spherical shells may be predicted with the high degree of accuracy normally required for the design of undersea vehicles. First, tests of accurately fabricated full spherical shells or deep spherical shells with ideal boundaries are needed to provide a reference. Then, tests of shells more representative of those encountered in engineering practice should be conducted to evaluate the weakening effects of initial imperfections, residual stresses, and adverse boundary conditions.

The series of tests described herein was designed to investigate the strength of accurately fabricated deep spherical shells with ideal boundaries and to provide a foundation for future experimental as well as theoretical treatment of the strength of spherical shells.

DESCRIPTION OF MODELS

Twenty-six structural models, consisting of hemispherical shells each bounded by a ring-stiffened cylinder, were machined from alumimum alloy bar stock. Thirteen models were machined from 6061-T6 alumimum alloy with a nominal yield strength of 43,000 psi and 13 models were machined from 7075-T6 alloy with a nominal yield strength of 80,000 psi. Young's modulus E for both materials, as determined by optical strain-gage measurements, was 10.8×10^6 psi. A Poisson's ratio ν of 0.3 in the elastic range was assumed. Table 1 gives the nominal model dimensions, and Table 2 presents the measured thicknesses of the hemispherical shells of each model. Figure 1 shows typical stress-strain curves for the material used. The ratios of secant modulus E_s and tangent modulus E_t to Young's modulus at various stress levels for the material used in each model are presented in Table 3.

TABLE 1

Nominal Model Dimensions

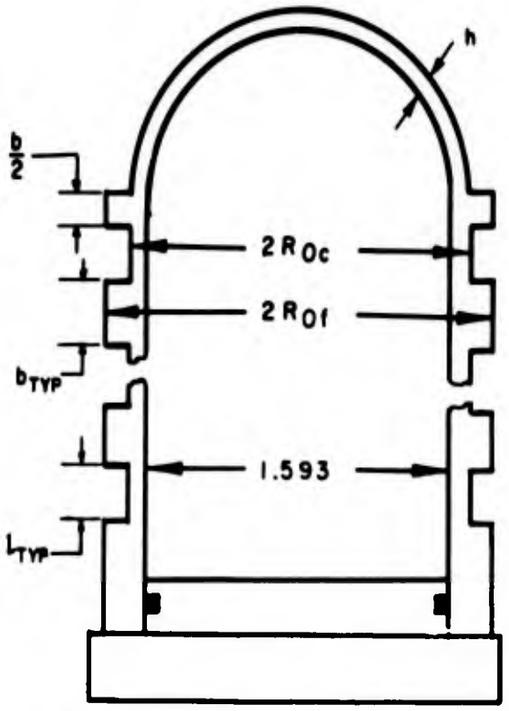

Model	Aluminum Alloy	h in.	b in.	$b/2$ in.	l in.	$2R_{Oc}$ in.	$2R_{Of}$ in.	Number of "l's"
A	6061-T6	0.0098	0.056	0.028	0.056	1.616	1.670	4
B		0.0100	0.056	0.028	0.056	1.616	1.670	4
C		0.0202	0.080	0.040	0.080	1.639	1.749	9
D		0.0202	0.080	0.040	0.080	1.639	1.749	9
E		0.0341	0.106	0.053	0.106	1.674	1.890	7
F		0.0345	0.106	0.053	0.106	1.674	1.890	7
G		0.0494	0.128	0.064	0.128	1.709	2.039	6
H		0.0494	0.128	0.064	0.128	1.709	2.039	6
I		0.062	0.148	0.074	0.148	1.747	2.245	6
II		0.066	0.148	0.074	0.148	1.747	2.245	6
J		0.064	0.148	0.074	0.148	1.747	2.245	6
K		0.079	0.344	0.172	0.172	1.800	2.230	3
L		0.081	0.344	0.172	0.172	1.800	2.230	3
M	7079-T6	0.0076	0.047	0.024	0.047	1.630	1.667	4
N		0.0077	0.047	0.024	0.047	1.630	1.667	4
O		0.0100	0.056	0.028	0.056	1.616	1.670	4
OO		0.0096	0.056	0.028	0.056	1.630	1.700	4
P		0.0106	0.056	0.028	0.056	1.616	1.670	4
Q		0.0190	0.080	0.040	0.080	1.639	1.749	9
R		0.0195	0.080	0.040	0.080	1.639	1.749	9
S		0.0335	0.106	0.053	0.106	1.674	1.890	7
T		0.0345	0.106	0.053	0.106	1.674	1.890	7
U		0.0490	0.128	0.064	0.128	1.709	2.039	6
V		0.0498	0.128	0.064	0.128	1.709	2.039	6
W		0.064	0.148	0.074	0.148	1.747	2.245	6
X		0.064	0.148	0.074	0.148	1.747	2.245	6

TABLE 2

Maximum and Minimum Measured Hemispherical Wall Thicknesses

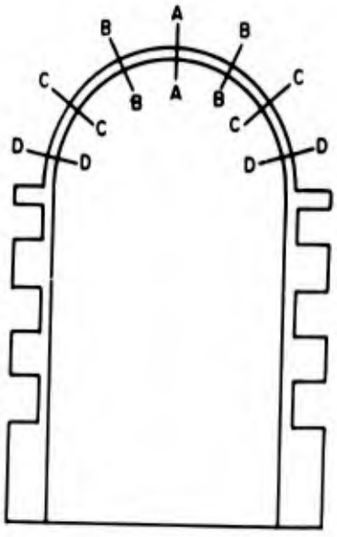

Model	Hemispherical Wall Thickness in Inches						
	A	B		C		D	
		Maximum	Minimum	Maximum	Minimum	Maximum	Minimum
A	0.0098	0.0098	0.0096	0.0100	0.0097	0.0102	0.0097
B	0.0101	0.0102	0.0100	0.0102	0.0098	0.0113	0.0110
C	0.0200	0.0206	0.0205	0.0205	0.0200	0.0206	0.0200
D	0.0200	0.0205	0.0200	0.0202	0.0200	0.0200	0.0195
E	0.0350	0.0332	0.0332	0.0345	0.0341	0.0350	0.0345
F	0.0350	0.0345	0.0338	0.0351	0.0348	0.0352	0.0352
G	0.0502	0.0495	0.0493	0.0495	0.0493	0.0510	0.0500
H	0.0502	0.0495	0.0493	0.0495	0.0493	0.0500	0.0496
I	0.063	0.062	0.062	0.062	0.062	0.065	0.065
II	0.066	0.066	0.066	0.067	0.067	0.068	0.068
J	0.064	0.064	0.064	0.064	0.064	0.065	0.065
K	0.079	0.079	0.078	0.082	0.082	0.083	0.082
L	0.080	0.081	0.081	0.082	0.082	0.083	0.083
M	0.0079	0.0075	0.0073	0.0081	0.0072	0.0078	0.0066
N	0.0075	0.0078	0.0078	0.0081	0.0073	0.0087	0.0083
O	0.0100	0.0099	0.0098	0.0108	0.0105	0.0109	0.0105
OO	0.0094	0.0100	0.0100	0.0095	0.0094	0.0103	0.0097
P	0.0101	0.0112	0.0111	0.0115	0.0119	0.0111	0.0111
Q	0.0190	0.0192	0.0186	0.0211	0.0205	0.0215	0.0209
R	0.0200	0.0192	0.0190	0.0205	0.0202	0.205	0.0198
S	0.0340	0.0338	0.0325	0.0338	0.0332	0.0338	0.0335
T	0.0350	0.0340	0.0338	0.0352	0.0350	0.0356	0.0354
U	0.0496	0.0488	0.0480	0.0496	0.0494	0.0499	0.0496
V	0.0504	0.0495	0.0490	0.0510	0.0505	0.0519	0.0515
W	0.065	0.063	0.063	0.064	0.064	0.067	0.067
X	0.065	0.063	0.063	0.064	0.064	0.066	0.066

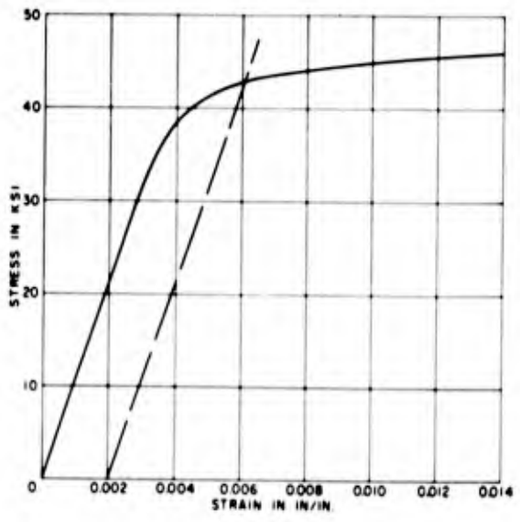

1a - 6061 - T6 Aluminum Alloy

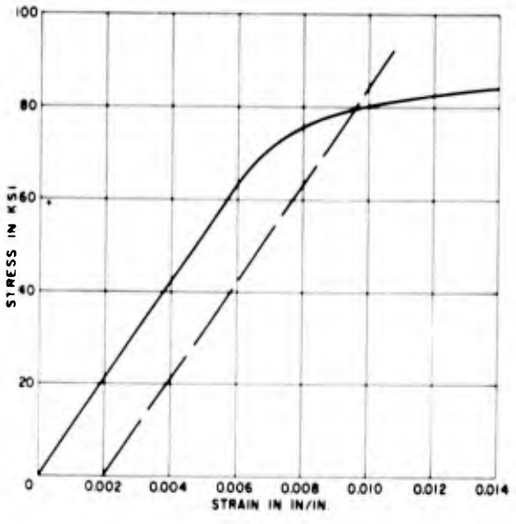

1b - 7075 - T6 Aluminum Alloy

Figure 1 - Typical Stress-Strain Curves for Material Used

TABLE 3

Ratios of Secant Modulus and Tangent Modulus to Young's Modulus

Table 3a - 6061 - T6 Aluminum Alloy

Model	Stress in psi																									
	35,000		36,000		37,000		38,000		39,000		4 ,000		41,000		42,000		43,000		44,000		45,000		46,000		47,000		48,000	
	E_t/E	E_s/E	E_t/E	E_s/E	E_t/E	E_s/E	E_t/E	E_s/E	E_t/E	E_s/E	E_t/E	E_s/E	E_t/E	E_s/E	E_t/E	E_s/E	E_t/E	E_s/E	E_t/E	E_s/E	E_t/E	E_s/E	E_t/E	E_s/E	E_t/E	E_s/E	E_t/E	E_s/E
A	1.00	1.00	0.94	0.99	0.82	0.98	0.64	0.96	0.51	0.93	0.41	0.90	0.30	0.87	0.22	0.83	0.16	0.75	0.094	0.67	0.058	0.57	0.046	0.47	0.46	0.39	0.046	0.33
B	1.00	1.00	0.96	0.99	0.86	0.98	0.73	0.97	0.59	0.96	0.46	0.93	0.36	0.90	0.27	0.86	0.19	0.81	0.12	0.72	0.066	0.63	0.049	0.52	0.049	0.42	0.049	0.37
C	1.00	1.00	0.98	1.00	0.90	0.99	0.70	0.96	0.48	0.94	0.32	0.90	0.20	0.88	0.14	0.79	0.084	0.69	0.043	0.57	0.042	0.44	0.042	0.36	0.042	0.30	0.042	0.26
D	1.00	1.00	0.98	1.00	0.90	0.99	0.70	0.96	0.48	0.94	0.32	0.91	0.20	0.88	0.14	0.79	0.084	0.69	0.043	0.57	0.042	0.44	0.042	0.36	0.042	0.30	0.042	0.26
E	1.00	1.00	0.96	1.00	0.84	0.98	0.66	0.96	0.52	0.94	0.41	0.91	0.31	0.88	0.23	0.83	0.17	0.76	0.11	0.69	0.062	0.58	0.048	0.49	0.048	0.40	0.048	0.35
F	1.00	1.00	0.98	1.00	0.86	0.99	0.68	0.97	0.54	0.95	0.41	0.92	0.32	0.88	0.23	0.84	0.18	0.77	0.12	0.70	0.067	0.60	0.049	0.51	0.049	0.41	0.049	0.36
G	1.00	1.00	0.98	1.00	0.86	0.99	0.68	0.97	0.54	0.95	0.41	0.92	0.32	0.88	0.23	0.84	0.18	0.77	0.12	0.70	0.067	0.60	0.049	0.51	0.049	0.41	0.049	0.36
H	1.00	1.00	0.97	1.00	0.86	0.99	0.70	0.97	0.56	0.95	0.44	0.93	0.34	0.89	0.25	0.85	0.19	0.79	0.12	0.71	0.066	0.61	0.049	0.51	0.049	0.42	0.049	0.36
I	1.00	1.00	0.95	0.99	0.86	0.98	0.75	0.97	0.61	0.96	0.50	0.94	0.38	0.91	0.28	0.87	0.20	0.83	0.12	0.73	0.065	0.64	0.049	0.53	0.049	0.43	0.049	0.37
II	1.00	1.00	0.90	0.99	0.69	0.98	0.57	0.95	0.43	0.92	0.34	0.89	0.26	0.86	0.14	0.77	0.090	0.70	0.053	0.56	0.037	0.44	0.030	0.35	0.030	0.28	0.030	0.23
J	1.00	1.00	0.95	0.99	0.86	0.98	0.75	0.97	0.61	0.96	0.50	0.94	0.38	0.91	0.28	0.87	0.20	0.83	0.12	0.73	0.065	0.64	0.049	0.53	0.049	0.43	0.049	0.37
K	0.99	1.00	0.95	0.99	0.86	0.98	0.75	0.97	0.61	0.95	0.50	0.93	0.38	0.90	0.29	0.87	0.21	0.82	0.13	0.73	0.071	0.63	0.047	0.53	0.047	0.43	0.047	0.36
L	0.98	1.00	0.95	0.99	0.85	0.98	0.75	0.96	0.61	0.94	0.49	0.92	0.38	0.90	0.29	0.87	0.21	0.81	0.14	0.73	0.076	0.62	0.045	0.53	0.045	0.43	0.045	0.36

Table 3b - 7075 - T6 Aluminum Alloy

Model	Stress in psi																									
	60,000		62,000		64,000		66,000		68,000		70,000		72,000		74,000		76,000		78,000		80,000		82,000		84,000		86,000	
	E_t/E	E_s/E	E_t/E	E_s/E	E_t/E	E_s/E	E_t/E	E_s/E	E_t/E	E_s/E	E_t/E	E_s/E	E_t/E	E_s/E	E_t/E	E_s/E	E_t/E	E_s/E	E_t/E	E_s/E	E_t/E	E_s/E	E_t/E	E_s/E	E_t/E	E_s/E	E_t/E	E_s/E
M	1.00	1.00	1.00	1.00	1.00	1.00	0.90	0.99	0.81	0.97	0.69	0.95	0.58	0.94	0.47	0.91	0.35	0.89	0.27	0.84	0.18	0.76	0.11	0.68	0.080	0.60	0.080	0.52
N	1.00	1.00	1.00	1.00	1.00	1.00	0.90	0.99	0.81	0.97	0.69	0.95	0.58	0.94	0.47	0.91	0.35	0.89	0.27	0.84	0.18	0.76	0.11	0.68	0.080	0.60	0.080	0.52
O	1.00	1.00	1.00	1.00	0.95	0.99	0.88	0.98	0.77	0.96	0.67	0.95	0.56	0.93	0.44	0.91	0.34	0.88	0.26	0.84	0.18	0.77	0.13	0.71	0.076	0.62	0.070	0.53
OO	1.00	1.00	1.00	1.00	1.00	1.00	0.90	0.99	0.81	0.97	0.69	0.95	0.58	0.94	0.47	0.91	0.35	0.89	0.27	0.84	0.18	0.76	0.11	0.68	0.080	0.60	0.080	0.52
P	0.95	1.00	0.88	0.99	0.76	0.97	0.65	0.95	0.53	0.93	0.40	0.90	0.29	0.87	0.21	0.81	0.16	0.73	0.11	0.64	0.078	0.55	0.070	0.48	0.070	0.42	0.070	0.37
Q	0.97	1.00	0.92	0.99	0.82	0.98	0.71	0.96	0.61	0.94	0.49	0.91	0.38	0.89	0.29	0.84	0.22	0.78	0.16	0.71	0.11	0.63	0.090	0.55	0.072	0.49	0.070	0.43
R	0.95	1.00	0.88	0.99	0.76	0.97	0.65	0.95	0.53	0.93	0.40	0.90	0.29	0.87	0.21	0.81	0.16	0.73	0.11	0.64	0.078	0.55	0.070	0.48	0.070	0.42	0.070	0.37
S	0.97	1.00	0.92	0.99	0.84	0.98	0.72	0.97	0.62	0.95	0.50	0.91	0.39	0.88	0.30	0.84	0.23	0.78	0.17	0.70	0.089	0.63	0.081	0.55	0.079	0.49	0.073	0.43
T	0.98	1.00	0.96	1.00	0.92	0.99	0.80	0.98	0.71	0.97	0.61	0.93	0.49	0.90	0.38	0.87	0.29	0.83	0.22	0.76	0.16	0.70	0.11	0.63	0.088	0.56	0.075	0.53
U	1.00	1.00	1.00	1.00	1.00	1.00	0.88	0.99	0.80	0.98	0.71	0.95	0.59	0.92	0.47	0.90	0.36	0.88	0.28	0.82	0.20	0.78	0.14	0.70	0.097	0.62	0.078	0.54
V	1.00	1.00	1.00	1.00	0.97	1.00	0.91	0.98	0.83	0.97	0.66	0.95	0.52	0.93	0.38	0.89	0.28	0.86	0.19	0.80	0.11	0.71	0.075	0.61	0.075	0.53	0.075	0.46
W	1.00	1.00	1.00	1.00	0.99	1.00	0.89	0.99	0.81	0.98	0.69	0.95	0.57	0.92	0.44	0.90	0.33	0.87	0.25	0.81	0.17	0.76	0.12	0.67	0.090	0.59	0.077	0.51
X	1.00	1.00	1.00	1.00	0.98	1.00	0.90	0.99	0.82	0.97	0.68	0.95	0.54	0.92	0.41	0.89	0.31	0.86	0.22	0.81	0.14	0.74	0.096	0.64	0.082	0.56	0.076	0.49

Each model was machined in an identical manner. First, the inside contour was machined by using a form tool; then, the exterior surface of each spherical shell was obtained by using a lathe with a ball-turning attachment. Finally, the exterior surface of the ring-stiffened cylinder was machined.

The stiffened cylindrical portions of all models except Models M, N, and OO were designed to provide conditions of membrane deflection and no rotation at the edge of their respective hemispherical ends.[11] The cylinders of these models were considerably more rigid than the cylinders provided by those boundaries which give rise to membrane deformations.

TEST PROCEDURE AND RESULTS

Each model was tested under external hydrostatic pressure. Pressure tanks of different sizes were used since the tests were conducted over a period of several months and no single facility was available throughout this time. Pressure was applied in increments and each new pressure level was held at least 1 min. The final pressure increment was normally less than 2 percent of the collapse pressure. Every effort was made to minimize any pressure surge when applying load. Some models failed under constant load whereas others collapsed while pressure was being applied.

Table 4 presents the experimental collapse pressures. Photographs of the models after collapse are shown in Figure 2. Model E could not be located after the test and, consequently, is not shown in Figure 2.

DISCUSSION

ELASTIC-INSTABILITY MODELS

The experimental collapse pressures of Models M, N, O, OO, and P, which collapsed at stress levels well within the elastic range of the material, are compared with the classical linear theory of Zoelly in Table 5. The ratios of experimental collapse pressure to theoretical collapse pressure shown in Table 5 are from two to three times greater than the ratios obtained in previous experiments by Sechler and Bollay[1] and by Klöppel and Jungbluth.[3] This confirms the suspicion that the low values of previously observed collapse pressure were caused mainly by initial imperfections, residual stresses, and adverse boundary conditions.

TABLE 4

Experimental Collapse Pressures

Model	Experimental Collapse Pressure, P_{EXP} psi
A	890
B	935
C	1,810
D	1,790
E	3,350
F	3,375
G	4,950
H	5,150
I	5,900
II	6,300
V	6,450
K	8,200
L	8,200
M	800
N	830
O	1,170
OO	1,230
P	1,215
Q	3,160
R	3,280
S	5,875
T	6,200
U	9,050
V	9,300
W	12,200
X	12,150

Figure 2 - Models After Collapse

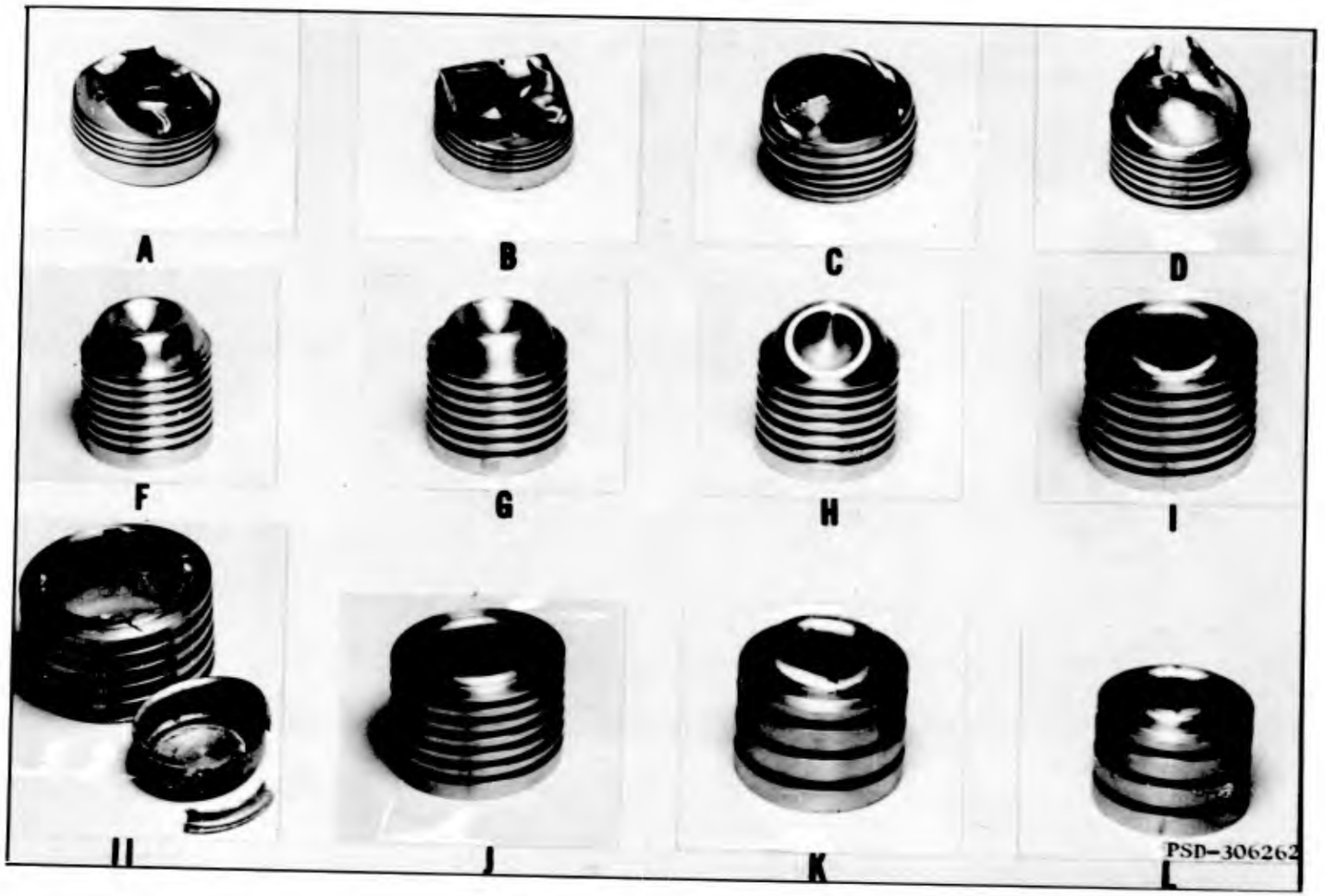

Figure 2a — 6061-T6 Aluminum Models

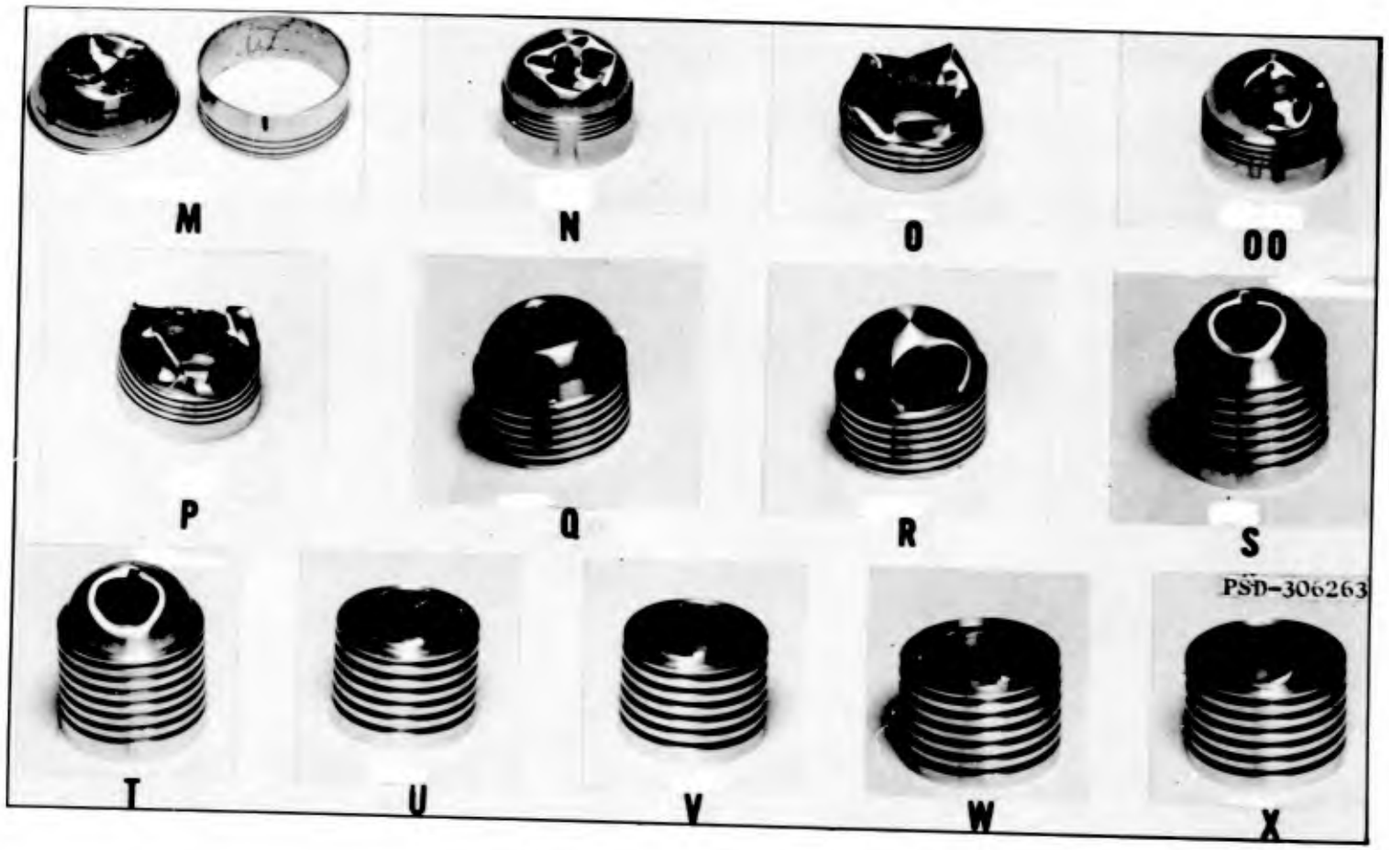

Figure 2b – 7079-T6 Aluminum Models

TABLE 5

Comparison of Experimental Elastic Collapse Pressures with Classical Theory

Model	Experimental Collapse Pressure, P_{EXP} psi	Average Shell Thickness, h in.	Mean Radius, R in.	Theoretical Collapse Pressure, $P_1 = 1.21E(h/R)^2$ psi	$\frac{P_{EXP}}{P_1}$
M	800	0.0076	0.800	1180	0.68
N	830	0.0077	0.801	1210	0.69
O	1170	0.0100	0.802	2030	0.58
OO	1230	0.0096	0.801	1875	0.66
P	1215	0.0106	0.802	2285	0.53

The machining of the shells in this series assured near perfect sphericity. Small initial departures from a true radius of curvature were observed in models tested by Klöppel and Jungbluth. Unfortunately, very little information on the model tested by Sechler and Bollay can be found in the literature. Although every effort was made to minimize variations in shell thickness for the series of models described herein, small variations were found to be unavoidable (see Table 2). The deviations in thickness from a mean value, however, were considerably less than the maximum value of 10 percent present in the models of Klöppel and Jungbluth.

Residual machining stresses were present since the models were not stress-relieved, but they are considered negligible. Appreciable residual stresses were present in the models reported in Reference 3 which were cold-formed.

The collapse strength of the spherical portion of Models M, N, and OO was not influenced by boundary conditions because their collapse occurred away from the boundaries. This indicated that the overdesign of the cylinder did not create serious edge effects. The definite lobar pattern shown by Models O and P after collapse suggested that the insufficient strength of their boundary cylinders lowered the collapse strength of thier spherical portion. This lobar pattern is typical of the general-instability collapse mode of cylinder and head. Unfortunately, there is no theory available to evaluate

the overall stability strength of these models and its effect on the collapse strength of the spherical portion. The strength of the deep spherical shells tested by Klöppel and Jungbluth was affected by the boundary conditions since collapse was initiated in the shell adjacent to the rigid support.

The experimental collapse strength of Models M, N, and OO was about 70 percent of the strength predicted by Zoelly. Because each Model tested had small deviations in shell thickness, this series of tests does not demonstrate conclusively the maximum elastic collapse strength of perfect spherical shells. These tests do show, however, that the lower buckling loads predicted by Von Kármán and Tsien may be greatly exceeded if the spherical shells are constructed with sufficient care and if, in the case of imcomplete spherical shells, satisfactory boundaries are provided.* It should be remembered that Von Kármán and Tsien considered their analysis applicable to shells with initial imperfections and, therefore, it is not surprising that the collapse strength of machined models should exceed that predicted by their analysis. To investigate further the maximum elastic buckling pressure attainable by experiment, it appears advantageous to test larger machined models in which unavoidable small variations in shell thickness would not be as critical.

INELASTIC-INSTABILITY MODELS

Table 6 compares the experimental collapse pressures for this series with the collapse pressures obtained from the inelastic-buckling solutions of Bijlaard,[8] Gerard,[9] and Lunchick[10] and from an empirical formula. The collapse pressures obtained from each of the solutions of Bijlaard, Gerard, and Lunchick may be expressed in the general form:

$$p_{B,G,L} = \eta\, p_1 \qquad [5]$$

---

*It is interesting to note that in Reference 5, Dr. Friedrichs solved the nonlinear problem based on a "boundary-layer theory" and obtained results which are in rather good agreement with this series of tests. His analysis, together with the analysis of Von Kármán and Tsien, assumes that the shell is deflected only parallel to the radial axis of symmetry. Unfortunately, Friedrichs proceeded to demonstrate that placing this restriction on deformations is in error and that, in the limiting linear case, it doubles the Zoelly load. By removing this restriction, Friedrichs obtained Zoelly's equation for the linear case but failed to obtain a solution for the nonlinear case.

where η is commonly called the plasticity reduction factor and p_l is the classical small deflection buckling pressure. The solution of Bijlaard is identical to that of Gerard for Poisson's ratio in the plastic range ν_p of 0.5. Their reduction factor $\eta_{B,G}$ may then be defined as

$$\eta_{B,G} = \left[(1-\nu^2)/(1-\nu_p^2) \right]^{1/2} \left(E_s/E\right) \left(E_t/E_s\right)^{1/2} \qquad [6]$$

and their solution for the collapse pressure $p_{B,G}$ then becomes

$$p_{B,G} = 1.154 \sqrt{\frac{E_s E_t}{(1-\nu_p{}^2)}} \left(\frac{h}{R}\right)^2 \qquad [7]$$

Lunchick considered a variable Poisson's ratio in the plastic range. His reduction factor η_L may be defined as

$$\eta_L = \left[(1-\nu^2)/(1-\nu_t)(1+\nu_s) \right]^{1/2} \left(E_s/E\right)\left(E_t/E_s\right)^{1/2} \qquad [8]$$

where $$\nu_t = 1/2-(1/2-\nu)E_{t/E}$$

and $$\nu_s = 1/2-(1/2-\nu)E_{s/E}$$

and his solution for the collapse pressure p_L becomes

$$p_L = 1.154 \sqrt{\frac{E_s\ E_t}{(1-\nu_t)(1+\nu_s)}} \left(\frac{h}{R}\right)^2 \qquad [9]$$

For this series of tests there is no significant difference between the pressures obtained from Equations [7] and [9]; each gives pressures somewhat greater than those observed; see Table 6. These results appear to have been anticipated by both Gerard[9] and Lunchick[10] since each suggested that his reduction factor could also be used to modify large deflection theory in the inelastic region and thereby obtain somewhat lower collapse pressures. Unfortunately, in the elastic region no reliable large deflection theory appears to be available for the geometries studied.

The empirical method, also used in Table 6 to predict collapse pressures, is derived as follows: If the average tangential buckling stress σ_{AVE} is defined from equilibruim as

$$\sigma_{AVE} = \frac{p_3 R_0^2}{2 Rh} \qquad [10]$$

where R_0 is the radius to the outer surface of the shell, the observed elastic collapse strengths of Models M, N, and OO may be approximated by

$$p_3 = \frac{0.8}{\sqrt{(1-\nu^2)}} E \left(\frac{h}{R_0}\right)^2 \qquad [11]$$

When the effects of a variable Poisson's ratio are neglected and the simple reduction factor

$$\eta_E = \sqrt{\frac{E_s E_t}{E^2}} \qquad [12]$$

is assumed,

an empirical expression for the inelastic collapse pressure p_E may be given in the same form as Equation [5]; namely,

$$p_E = \eta_E p_3 \qquad [13]$$

or

$$p_E = 0.8\sqrt{\frac{E_s E_t}{(1-\nu^2)}}\left(\frac{h}{R_0}\right)^2 \qquad [14]$$

Table 6 shows that the experimental results are in good agreement with those calculated by using Equation [14].

Since the only difference between $\eta_{B,G}$, η_L, and η_E is the treatment of Poisson's ratio in the plastic range, it is apparent that similar results would be obtained if p_3 were substituted for p_1 in Equation [5]. It is significant that for this series of tests, which covers thickness to radius ratios from about 1/10 to 1/100, the elastic-buckling coefficient remains constant. This is in total agreement with the existing inelastic theories.[8,9,10] Therefore, the cause for disagreement between this series of tests and existing inelastic theory can be attributed to the magnitude of the constant elastic-buckling ceofficient. Specifically, for an elastic Poisson's ratio of 0.3, the elastic-buckling coefficient of about 0.84 is obtained for this series of experiments; whereas each available inelastic theory assumes the classical elastic-buckling coefficient of 1.21; see Equations [3] and [5].

TABLE 6

Comparison of Experimental Collapse Pressures with Inelastic Theory

Model	P_{EXP} psi	$\frac{P_{EXP}}{P_{B,G} = 1.154\sqrt{\frac{E_S E_T}{(1-\nu_P^2)}}\left(\frac{h}{R}\right)^2}$	$\frac{P_{EXP}}{P_L = 1.154\sqrt{\frac{E_S E_T}{(1-\nu_T)(1+\nu_S)}}\left(\frac{h}{R}\right)^2}$	$\frac{P_{EXP}}{P_E = 0.8\sqrt{\frac{E_S E_T}{1-\nu^2}}\left(\frac{h}{R_O}\right)^2}$
A	890	0.89	0.89	0.95
B	935	0.89	0.89	0.96
C	1810	0.84	0.84	0.89
D	1790	0.83	0.83	0.88
E	3350	0.87	0.87	0.94
F	3375	0.86	0.86	0.93
G	4950	0.82	0.82	0.96
H	5150	0.86	0.86	0.99
I	5900	0.77	0.77	0.89
II	6300	0.83	0.83	0.95
J	6450	0.80	0.80	0.94
K	8200	0.83	0.83	0.96
L	8200	0.80	0.80	0.94
M*	800	0.68	0.68	0.99
N*	830	0.69	0.69	1.00
O*	1170	0.67	0.67	0.84
OO*	1230	0.73	0.74	0.96
P*	1215	0.68	0.68	0.78
Q	3160	0.89	0.89	0.94
R	3280	0.92	0.92	1.00
S	5875	0.90	0.90	0.97
T	6200	0.89	0.89	0.98
U	9050	0.88	0.88	0.98
V	9300	0.91	0.91	1.02
W	12,200	0.88	0.88	1.02
X	12,150	0.87	0.87	1.02

* Elastic Failure.

APPLICATION OF TEST RESULTS

The results of these tests will probably be of little direct value to the naval architect since it is not practical to machine most spherical shells encountered in engineering practice. All but a few of the smaller shells will probably be formed by spinning or by pressing segments to the proper shape and then welding them together. In either case, considerable departure from sphericity will exist, although in this series of models good sphericity was assured because of machining the contours. Large variations in thickness can also be expected in practice, particularly if the shells are formed by spinning. Spherical shells formed by spinning or pressing will also have considerable residual stresses unless stress-relieved and not entirely uniform yield strengths. These residual stresses will cause early inelastic behavior in the shell which will, in turn, lower the collapse strength. Furthermore, ideal boundary conditions are not practical for many deep spherical shells. An example of this impracticality is the normally unacceptable weight penalty imposed by providing ideal boundaries for a hemisphere used to close off the end of a cylindrical hull. This penalty is due to the appreciably greater radial deflection of a cylinder when compared to a sphere operating at similar stress levels. In practice, most spherical shells will have penetrations. However, their effect on collapse strength has not been considered in these tests.

These tests are valuable, however, because they demonstrate the collapse pressures that can be expected for accurately machined spherical shells. In this respect, they may be considered as an upper bound for experimental collapse pressures. Therefore, they can serve as a reference to which future tests on spun or pressed spherical shells may be compared to determine the detrimental effects of initial departures from sphericity, variations in shell thicknesses, residual stresses, adverse boundary conditions, and penetrations.

CONCLUSIONS

The following conclusions are made concerning the hydrostatic strength of the spherical portions of the models tested:

1. The ratios of experimental elastic collapse pressure to the pressure obtained from the classical linear theory of Zoelly were from two to three

times greater than the ratios for previous tests recorded in the literature. This large increase was achieved by machining the shells rather than by forming them from a flat plate and by eliminating adverse boundary conditions.

2. The observed collapse pressures in the elastic range could not be predicted by either the classical linear theory of Zoelly or any of the available large deflection theories. The maximum collapse pressure obtained was about 70 percent of the pressure predicted by Zoelly.

3. For each model tested, the available theories of inelastic instability of Bijlaard, Gerard, and Lunchick gave collapse pressures higher than the corresponding experimental collapse pressures.

4. The collapse strength of those models which failed at stress levels above the proportional limit may be predicted by an empirical formula based on the observed collapse strength of the elastic models and a plasticity reduction factor similar to that developed in existing theory.

RECOMMENDATIONS

1. Tests of spherical shells formed both by spinning and by pressing should be conducted to evaluate the effects of initial imperfections and residual stresses on collapse strength.

2. The effect of boundary conditions and penetration on the collapse strength of spherical shells should be investigated.

ACKNOWLEDGMENTS

The author acknowledges the contributions of Mr. Rollin P. Mead of the Industrial Department, who supervised the machining of the models and the assistance of Mr. Leonard J. Giuffreda, who conducted the hydrostatic tests.

APPENDIX

OBSERVATIONS ON PLASTIC SPHERES UNDER UNIFORM PRESSURE

Prior to this present work, two small plastic spheres were collapsed under external pressure. The objectives of these exploratory tests were to investigate the applicability of Tsien's "energy criterion of jump" and to obtain high-speed photographs of the collapse of spherical shells.

In the first experiment, a plastic sphere was subjected to alternating static loads of hydrostatic and air pressure to determine whether the energy in the pressure vessel influences collapse pressure, as implied by the theory of Tsien.[7] The vessel in which hydrostatic pressure was applied was shaped to provide a minimum volume of water between the sphere and the wall of the vessel; see Figure 3. The volume of the vessel in which air pressure was applied was about 1000 times the volume of the other vessel; thus, it approached the "dead load" condition. Since the test was not intended for quantitative evaluation, no measurements of geometric or physical properties were made. The loading sequence and test results are shown in Table 7.

A second plastic sphere was subjected to external hydrostatic pressure in the vessel shown in Figure 3, and a high-speed camera operating at an approximate rate of 3000 frames per second was used to record the collapse mechanism. Difficulty in synchronizing the camera with the collapse of the sphere was anticipated. Therefore, a similar sphere was first collapsed and the buckling pressure was noted. Then the new sphere was placed in the test tank and subjected to a pressure slightly below the critical pressure. As the camera was started, additional pressure was applied to the sphere so that it collapsed while the camera was running. Figure 4 shows photographs of six consecutive frames covering a time period of about 0.002 second.

The following observations were made during the rather crude exploratory tests just described.

1. The collapse strength of the first plastic sphere, when tested in the small vessel under hydrostatic pressure, was not appreciably greater than its strength in a relative large vessel under air pressure.

2. The collapse of the second sphere began as a small inward dimple and reached its post-buckling configuration very rapidly.

The first observation suggests that the collapse strength of complete spherical shells is not dependent on the volume or energy of the pressure vessel as implied by Tsien.[7] The fact that the collapse of the second sphere began as a single, small, inward dimple indicates that collapse strength is influenced by local effects of initial departures from sphericity, non uniform wall thickness, residual stresses due to fabrication, and, in the case of incomplete spheres, the effects of edge conditions. Outside dynamic disturbances may also have an effect on the collapse strength observed under normal laboratory, conditions, but it seems likely that this effect is small.

Figure 3 - Pressure Vessel Used for Applying Hydrostatic Pressure to Plastic Spheres

TABLE 7

Summary of Static Tests of a Small Plastic Sphere Under External Pressure

Load Number	Pressure Medium	Maximum Pressure psi	Remarks
1	Water	50	Maximum pressure held 1 min. No drop in pressure observed.
2	Air	50	Maximum pressure held 1 min. No drop in pressure observed.
3	Water	52 1/2	Collapsed after holding maximum pressure for 10 sec. A residual pressure of 13 psi was observed after collapse.
4	Water	40	Maximum pressure held 1 min. No drop in pressure observed.
5	Air	40	Maximum pressure held 1 min. No drop in pressure observed.
6	Water	42 1/2	Maximum pressure held 1 min. No drop in pressure observed.
7	Air	42 1/2	Maximum pressure held 1 min. No drop in pressure observed.
8	Water	43	Collapsed while applying pressure. A residual pressure of 14 psi was observed after collapse.
9	Air	45	Collapsed and ruptured while applying pressure.

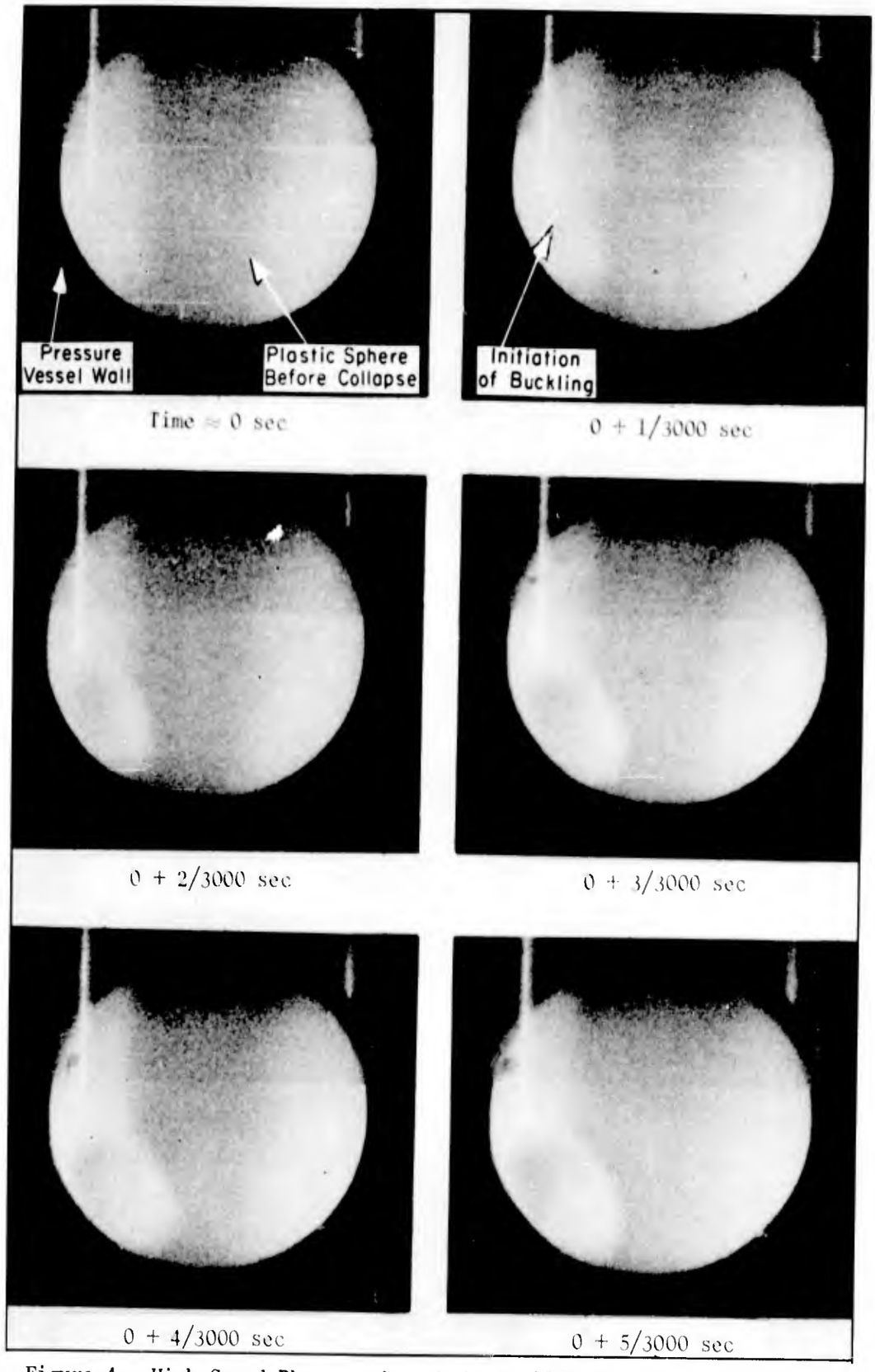

Figure 4 - High-Speed Photographs of the Buckling of a Plastic Sphere under Hydrostatic Pressure

REFERENCES

1. Fung, Y.C. and Sechler, E.E., "Instability of Thin Elastic Shells," Proceedings of the First Symposium on Naval Structural Mechanics (1960).

2. Timoshenko, S., "Theory of Elastic Stability," McGraw-Hill Book Co., Inc., New York (1936).

3. Klöppel, K. and Jungbluth, O., "Beitrag zum Durchschlagsproblem dunnwandiger Kugelschalen (Versuche und Bemessungsformeln), (Contribution to the Durchschlag-Problem in Thin-Walled Spherical Shells (Experiments and Design Formulas). Der Stahlbau, Jahrg. 22, Heft 6, Berlin (1953).

4. Von Karman, T. and Tsien, H.S., "The Buckling of Spherical Shells by External Pressure," Journal of the Aeronautical Sciences, Vol. 7, No. 2 (Dec 1939).

5. Friedrichs, K.O., "On the Minimum Buckling Load for Spherical Shells," Theodore von Karman Anniversary Volume CIT (1941).

6. Murray, F.J. and Wright F.W., "The Buckling of Thin Spherical Shells," Journal of the Aerospace Sciences, Vol. 28, No. 3 (Mar 1961).

7. Tsien, H.S., "A Theory for the Buckling of Thin Shells," Journal of the Aeronautical Sciences, Vol. 9, No. 10 (Aug 1942).

8. Bijlaard, P.P., "Theory and Tests on the Plastic Stability of Plates and Shells," Journal of the Aeronautical Sciences, Vol. 16, No. 9 (Sep 1949).

9. Gerard, G., "Plastic Stability Theory of Thin Shells," Journal of the Aeronautical Sciences, Vol. 24, No. 4 (Apr 1957).

10. Lunchick, M.E., "Plastic Buckling Pressure for Spherical Shells," David Taylor Model Basin Report 1493 (in preparation).

11. Krenzke, M.A., "Hydrostatic Tests of Conical Reducers between Cylinders with and without Stiffeners at the Cone-Cylinder Juncture," David Taylor Model Basin Report 1187 (Feb 1959).

INITIAL DISTRIBUTION

Copies	
16	CHBUSHIPS
	2 Sci & Res Sec (Code 442)
	1 Lab Mgt (Code 320)
	3 Tech Info Br (Code 335)
	1 Struc Mech, Hull Mat & Fab (Code 341A)
	1 Prelim Des Br (Code 420)
	1 Prelim Des Sec (Code 421)
	1 Ship Protec (Code 423)
	1 Hull Des Br (Code 440)
	1 Struc Sec (Code 443)
	2 Sub Br (Code 525)
	1 Hull Arrgt, Struc & Preserv (Code 633)
	1 Pres Ves Sec (Code 651F)
2	CHONR
	1 Struc Mech Br (Code 439)
	1 Undersea Programs (Code 466)
4	CNO
	1 Plans, Programs & Req Br (Op 311)
	1 Sub Program Br (Op 713)
	1 Tech Anal & Adv Gr (Op 07T)
	1 Tech Support Br (Op 725)
10	CDR, ASTIA
1	DIR, USNEES
1	CDR, USNOL
1	DIR, USNRL (Code 2027)
1	CO & DIR, USNUSL
1	CO & DIR, USNEL
1	CDR, USNOTS, China Lake
1	CO, USNUOS
2	NAVSHIPYD PTSMH
2	NAVSHIPYD MARE
1	NAVSHIPYD CHASN
1	SUPSHIP, Groton
1	EB Div, Gen Dyn Corp
1	SUPSHIP, Newport News
1	NNSB & DD Co
1	SUPSHIP, Pascagoula
1	Ingalls Shipbldg Corp

Copies	
1	SUPSHIP, Camden
1	New York Shipbldg
1	DIR DEF R & E, Attn: Tech Library
1	CO, USNROTC & NAVADMINU, MIT
1	O in C, PGSCOL, Webb
1	DIR, APL, Univ of Washington, Seattle
1	NAS, Attn: Comm on Undersea Warfare
1	Prof. J. Kempner, PIB
1	Prof. G. Gerard, NYU
1	Dr. E. Wenk, Jr., Office of Sp Asst for Sc & Tech, The White House
1	Dr. R. DeHart, SWRI
1	Mr. Leonard P. Zick, Chicago Bridge & Iron Co
1	Dean V.L. Salerno, Fairleigh Univ
1	Prof. E.O. Waters, Yale Univ
2	Mr. C.F. Larson, Sec, Welding Research Council

David Taylor Model Basin. Report 1601.
TESTS OF MACHINED DEEP SPHERICAL SHELLS UNDER EXTERNAL HYDROSTATIC PRESSURE, by Martin A. Krenzke. May 1962. iii, 28p. illus., tables, diagrs, refs. UNCLASSIFIED

Twenty-six structural models, consisting of hemispherical shells bound by ring-stiffened cylinders designed to provide ideal edge conditions, were machined from two aluminum alloys and collapsed under hydrostatic pressure. The models were designed to investigate both elastic and inelastic failures. The collapse pressure of those models which failed elastically could not be predicted by either the linear theory of Zoelly or any of the available large-deflection theories. When an empirical formula based on the observed elastic collapse pressures was used, the collapse pressure of those models which failed at stress levels above the proportional limit of the material could be

1. Spherical shells--Collapse--Model tests
I. Krenzke, Martin A.
II. S-F013 03 02

David Taylor Model Basin. Report 1601.
TESTS OF MACHINED DEEP SPHERICAL SHELLS UNDER EXTERNAL HYDROSTATIC PRESSURE, by Martin A. Krenzke. May 1962. iii, 28p. illus., tables, diagrs, refs. UNCLASSIFIED

Twenty-six structural models, consisting of hemispherical shells bound by ring-stiffened cylinders designed to provide ideal edge conditions, were machined from two aluminum alloys and collapsed under hydrostatic pressure. The models were designed to investigate both elastic and inelastic failures. The collapse pressure of those models which failed elastically could not be predicted by either the linear theory of Zoelly or any of the available large-deflection theories. When an empirical formula based on the observed elastic collapse pressures was used, the collapse pressure of those models which failed at stress levels above the proportional limit of the material could be

1. Spherical shells--Collapse--Model tests
I. Krenzke, Martin A.
II. S-F013 03 02

David Taylor Model Basin. Report 1601.
TESTS OF MACHINED DEEP SPHERICAL SHELLS UNDER EXTERNAL HYDROSTATIC PRESSURE, by Martin A. Krenzke. May 1962. iii, 28p. illus., tables, diagrs, refs. UNCLASSIFIED

Twenty-six structural models, consisting of hemispherical shells bound by ring-stiffened cylinders designed to provide ideal edge conditions, were machined from two aluminum alloys and collapsed under hydrostatic pressure. The models were designed to investigate both elastic and inelastic failures. The collapse pressure of those models which failed elastically could not be predicted by either the linear theory of Zoelly or any of the available large-deflection theories. When an empirical formula based on the observed elastic collapse pressures was used, the collapse pressure of those models which failed at stress levels above the proportional limit of the material could be

1. Spherical shells--Collapse--Model tests
I. Krenzke, Martin A.
II. S-F013 03 02

David Taylor Model Basin. Report 1601.
TESTS OF MACHINED DEEP SPHERICAL SHELLS UNDER EXTERNAL HYDROSTATIC PRESSURE, by Martin A. Krenzke. May 1962. iii, 28p. illus., tables, diagrs, refs. UNCLASSIFIED

Twenty-six structural models, consisting of hemispherical shells bound by ring-stiffened cylinders designed to provide ideal edge conditions, were machined from two aluminum alloys and collapsed under hydrostatic pressure. The models were designed to investigate both elastic and inelastic failures. The collapse pressure of those models which failed elastically could not be predicted by either the linear theory of Zoelly or any of the available large-deflection theories. When an empirical formula based on the observed elastic collapse pressures was used, the collapse pressure of those models which failed at stress levels above the proportional limit of the material could be

1. Spherical shells--Collapse--Model tests
I. Krenzke, Martin A.
II. S-F013 03 02

predicted with reasonable accuracy. The agreement between the experimental values and those obtained from this empirical formula is within + 2 and – 12 percent.

predicted with reasonable accuracy. The agreement between the experimental values and those obtained from this empirical formula is within + 2 and – 12 percent.

predicted with reasonable accuracy. The agreement between the experimental values and those obtained from this empirical formula is within + 2 and – 12 percent.

predicted with reasonable accuracy. The agreement between the experimental values and those obtained from this empirical formula is within + 2 and – 12 percent.

David Taylor Model Basin. Report 1601.
TESTS OF MACHINED DEEP SPHERICAL SHELLS UNDER EXTERNAL HYDROSTATIC PRESSURE, by Martin A. Krenzke. May 1962. iii, 28p. illus., tables, diagrs, refs. UNCLASSIFIED

Twenty-six structural models, consisting of hemispherical shells bound by ring-stiffened cylinders designed to provide ideal edge conditions, were machined from two aluminum alloys and collapsed under hydrostatic pressure. The models were designed to investigate both elastic and inelastic failures. The collapse pressure of those models which failed elastically could not be predicted by either the linear theory of Zoelly or any of the available large-deflection theories. When an empirical formula based on the observed elastic collapse pressures was used, the collapse pressure of those models which failed at stress levels above the proportional limit of the material could be

1. Spherical shells--Collapse--Model tests
I. Krenzke, Martin A.
II. S-F013 03 02

David Taylor Model Basin. Report 1601.
TESTS OF MACHINED DEEP SPHERICAL SHELLS UNDER EXTERNAL HYDROSTATIC PRESSURE, by Martin A. Krenzke. May 1962. iii, 28p. illus., tables, diagrs, refs. UNCLASSIFIED

Twenty-six structural models, consisting of hemispherical shells bound by ring-stiffened cylinders designed to provide ideal edge conditions, were machined from two aluminum alloys and collapsed under hydrostatic pressure. The models were designed to investigate both elastic and inelastic failures. The collapse pressure of those models which failed elastically could not be predicted by either the linear theory of Zoelly or any of the available large-deflection theories. When an empirical formula based on the observed elastic collapse pressures was used, the collapse pressure of those models which failed at stress levels above the proportional limit of the material could be

1. Spherical shells--Collapse--Model tests
I. Krenzke, Martin A.
II. S-F013 03 02

David Taylor Model Basin. Report 1601.
TESTS OF MACHINED DEEP SPHERICAL SHELLS UNDER EXTERNAL HYDROSTATIC PRESSURE, by Martin A. Krenzke. May 1962. iii, 28p. illus., tables, diagrs, refs. UNCLASSIFIED

Twenty-six structural models, consisting of hemispherical shells bound by ring-stiffened cylinders designed to provide ideal edge conditions, were machined from two aluminum alloys and collapsed under hydrostatic pressure. The models were designed to investigate both elastic and inelastic failures. The collapse pressure of those models which failed elastically could not be predicted by either the linear theory of Zoelly or any of the available large-deflection theories. When an empirical formula based on the observed elastic collapse pressures was used, the collapse pressure of those models which failed at stress levels above the proportional limit of the material could be

1. Spherical shells--Collapse--Model tests
I. Krenzke, Martin A.
II. S-F013 03 02

David Taylor Model Basin. Report 1601.
TESTS OF MACHINED DEEP SPHERICAL SHELLS UNDER EXTERNAL HYDROSTATIC PRESSURE, by Martin A. Krenzke. May 1962. iii, 28p. illus., tables, diagrs, refs. UNCLASSIFIED

Twenty-six structural models, consisting of hemispherical shells bound by ring-stiffened cylinders designed to provide ideal edge conditions, were machined from two aluminum alloys and collapsed under hydrostatic pressure. The models were designed to investigate both elastic and inelastic failures. The collapse pressure of those models which failed elastically could not be predicted by either the linear theory of Zoelly or any of the available large-deflection theories. When an empirical formula based on the observed elastic collapse pressures was used, the collapse pressure of those models which failed at stress levels above the proportional limit of the material could be

1. Spherical shells--Collapse--Model tests
I. Krenzke, Martin A.
II. S-F013 03 02

predicted with reasonable accuracy. The agreement between the experimental values and those obtained from this empirical formula is within + 2 and – 12 percent.

predicted with reasonable accuracy. The agreement between the experimental values and those obtained from this empirical formula is within + 2 and – 12 percent.

predicted with reasonable accuracy. The agreement between the experimental values and those obtained from this empirical formula is within + 2 and – 12 percent.

predicted with reasonable accuracy. The agreement between the experimental values and those obtained from this empirical formula is within + 2 and – 12 percent.

UNCLASSIFIED